# Phase Transitions and CO2 Adsorption Properties of Polymeric Magnesium Formate

**ARTICLE** *in* CRYSTAL GROWTH & DESIGN · AUGUST 2008

Impact Factor: 4.89 · DOI: 10.1021/cg800181q



**9 AUTHORS**, INCLUDING:

Andrea Rossin
Italian National Research Council
**61** PUBLICATIONS **1,104** CITATIONS
SEE PROFILE

Luca Gonsalvi
Italian National Research Council
**103** PUBLICATIONS **2,348** CITATIONS
SEE PROFILE

Paolo Fornasiero
Università degli Studi di Trieste
**238** PUBLICATIONS **8,987** CITATIONS
SEE PROFILE

Maurizio Peruzzini
Italian National Research Council
**357** PUBLICATIONS **8,493** CITATIONS
SEE PROFILE

CRYSTAL GROWTH & DESIGN
2008
VOL. 8, NO. 9
3302–3308

# Phase Transitions and $CO_2$ Adsorption Properties of Polymeric Magnesium Formate

Andrea Rossin,[†] Andrea Ienco,[†] Ferdinando Costantino,[‡] Tiziano Montini,[§] Barbara Di Credico,[†] Maria Caporali,[†] Luca Gonsalvi,[†] Paolo Fornasiero,[§] and Maurizio Peruzzini*[,†]

*Consiglio Nazionale delle Ricerche, Istituto di Chimica dei Composti Organometallici (ICCOM-CNR), Via Madonna del Piano 10, 50019 Sesto Fiorentino (Firenze), Italy, Dipartimento di Chimica e CEMIN, Università di Perugia, via Elce di Sotto 8, 06123, Perugia, Italy, and Dipartimento di Scienze Chimiche, Università di Trieste, CENMAT, INSTM-Trieste and Unità associata ICCOM-CNR, Trieste, via L. Giorgieri 1, 34127 Trieste, Italy*

*Received February 17, 2008; Revised Manuscript Received May 1, 2008*

**ABSTRACT:** The solvothermal reaction of magnesium(II) salts with formic acid in *N,N*-dimethylformamide/$H_2O$ at 140 °C for 24 h afforded two different polymeric magnesium(II) formates, depending on the relative DMF/$H_2O$ content. A trigonal (space group $R\bar{3}c$) anhydrous phase $Mg(HCOO)_2(HCOOH) \supset (CH_3)_2NH$ (**1**) is formed under "dilute" conditions, while the orthorhombic (space group *Pbca*) dihydrate $Mg(HCOO)_2 \cdot 2H_2O$ (**2**) is the main product when the water content is higher. When **2** is dehydrated at 300 °C and subsequently exposed to water vapors, a quasi-reversible phase transition was observed, leading to a different polymorph of the same species (**2a**, monoclinic, space group $P2_1/c$). The process was entirely followed by X-ray powder diffraction (XRPD) at variable temperatures, and the same XRPD technique was used for structure solution and refinement of compound **2a**. Finally, $CO_2$ adsorption isotherms at ambient temperature were recorded for (preactivated) **2**, in order to test it as greenhouse gas storage material. A (promising) maximum value of 1.32 wt% $CO_2$ is stored under these conditions, but the *plateau* in the adsorption curve was not reached because of the higher carbon dioxide pressures required.

## Introduction

The research field of coordination polymers has undergone a relevant development in the last years, mainly due to the diverse potential applications of the materials synthesized. Beyond their magnetic,[1] catalytic,[2] and gas storage[3] properties, only in the recent literature reports on the host−guest behavior of these species have started to appear.[4]

At the same time, a boost on the study of polymeric metal formates in particular has been given by the discovery of a wide variety of crystalline phases that can be obtained with this simple and small organic linker.[5] Even though molecular formates have been known for a long time,[6] the technical applications described above, along with the necessity of finding new stable, cheap, and ready-to-use materials, have prompted researchers to re-examine the chemistry of these "classical" species.

The occurrence of polymorphism (different crystalline forms of the same compound) is not a rare event in crystal engineering;[7] the appearance of such a phenomenon is particularly likely when dealing with compounds that can be synthesized under different experimental conditions. In the field of metallorganic chemistry, very few examples are known[8] where, after solvent or guest removal and readsorption in a coordination network, a phase transition between polymorphs can take place. Retention of crystallinity during the process is usually only observed for systems displaying relatively *subtle variations* in the packing of molecules or in *rigid* three-dimensional (3D) framework materials.[9]

We report here on a novel 3D framework deriving from *anhydrous* magnesium formate, with a crystal structure isomorphous to the known zinc analogue $[(CH_3)_2NH_2][Zn(\mu\text{-}HCOO)_3]$.[10] In addition, a phase transition of magnesium formate *dihydrate* $[Mg(HCOO)_2 \cdot 2H_2O]$ has been discovered during the analysis of its dehydration−rehydration cycle carried out as a host−guest experiment using water as the guest molecule. Starting from an orthorhombic two-dimensional (2D) lamellar material, water removal followed by rehydration of the anhydrous phase so obtained, led to *different* 3D monoclinic microcrystals of the same compound. The overall process has been followed by single-crystal X-ray diffraction (XRD) and powder X-ray diffraction (XRPD),[11] infrared spectroscopy (FT-IR), and thermogravimetric analysis-differential thermal analysis (TGA-DTA).

Finally, these compounds were tested as potential storage materials for use in the field of reduction of greenhouse gas emissions. $CO_2$ adsorption isotherms of the activated phase derived from $Mg(HCOO)_2 \cdot 2H_2O$ have been recorded, to understand whether it could have permanent porosity and therefore application as an efficient "$CO_2$ sponge". The availability of materials of this kind containing s- or p-block metals is particularly sought after, owing to their low molecular weights, making them more appealing for practical applications.

## Experimental Section

**Materials and Methods.** All starting materials and solvents were of analytical grade. They were purchased from Aldrich and used as received, without further purification.

Coupled thermogravimetric (TG) and differential thermal analysis (DTA) were performed with a Netzsch STA490C thermoanalyzer under a 20 mL $min^{-1}$ air flux with a heating rate of 5 °C $min^{-1}$.

IR spectra (KBr pellets) were recorded on a Perkin-Elmer Spectrum BX Series FT-IR spectrometer, in the range 4000−400 $cm^{-1}$.

Adsorption isotherms were recorded using a Micromeritics ASAP 2020 instrument. Prior to the measurements, the samples were degassed at the desired temperature (120 or 300 °C) using a heating rate of 1 °C $min^{-1}$, maintaining the final temperature for at least 24 h. $CO_2$ adsorption isotherms were recorded at 25 °C. Elemental analyses were carried out at the University of Florence, Organic Chemistry Department.

* Author to which correspondence should be addressed. E-mail: mperuzzini@iccom.cnr.it.
[†] Consiglio Nazionale delle Ricerche, Istituto di Chimica dei Composti Organometallici (ICCOM-CNR).
[‡] Università di Perugia.
[§] Università di Trieste.

10.1021/cg800181q CCC: $40.75 
Published on Web 08/16/2008

**Table 1. Crystal Data and Structure Refinement for 1**

| empirical formula | $C_5H_{11}NO_6Mg$ |
|---|---|
| formula weight | 205.46 |
| temperature | 293(2) K |
| wavelength | 0.71069 Å |
| crystal system | trigonal |
| space group | $R\bar{3}c$ |
| unit cell dimensions | $a = 8.149(3)$ Å<br>$c = 22.598(8)$ Å |
| volume | 1299.6(8) Å$^3$ |
| $Z$ | 6 |
| density (calculated) | 1.575 Mg/m$^3$ |
| absorption coefficient | 0.205 mm$^{-1}$ |
| $F(000)$ | 648 |
| crystal size | 0.02 × 0.015 × 0.01 mm$^3$ |
| theta range for data collection | 3.40 to 24.96° |
| index ranges | $-9 \le h \le 0$, $-4 \le k \le 9$,<br>$-26 \le l \le 14$ |
| reflections collected | 710 |
| independent reflections | 259 [R(int) = 0.0236] |
| completeness to theta = 24.96° | 100.0% |
| refinement method | full-matrix least-squares on $F^2$ |
| data/restraints/parameters | 259/0/22 |
| goodness-of-fit on $F^2$ | 1.445 |
| final $R$ indices [$I > 2\sigma(I)$] | $R_1 = 0.0430$, $wR_2 = 0.1160$ |
| $R$ indices (all data) | $R_1 = 0.0471$, $wR_2 = 0.1203$ |
| largest diff peak and hole | 0.488 and −0.284 e Å$^{-3}$ |

**Preparation of Magnesium(II) Formate $Mg(HCOO)_2(HCOOH) \supset (CH_3)_2NH$ (1).** Formic acid was employed directly as a reagent, instead of generating it from solvothermal decomposition of a more complex carboxylic acid.[10] In a typical experiment, magnesium perchlorate hexahydrate $Mg(ClO_4)_2 \cdot 6H_2O$ (1.76 g, 5.3 mmol) was dissolved together with formic acid (0.1 mL, 2.6 mmol) in a *N,N*-dimethylformamide (DMF)/ethanol/water mixture in the ratio 10 mL:0.5 mL:0.5 mL. The clear solution was transferred to a Teflon-lined stainless steel autoclave, sealed and heated under autogenous pressure at 140 °C for 24 h. After slow overnight cooling, colorless plate-like crystals of **1** were collected, washed with fresh ethanol (4 × 10 mL), and dried under a nitrogen stream at room temperature. Yield: 0.51 g (47%; calculated with respect to magnesium perchlorate). Anal. Calcd. for **1**, $C_5H_{11}NO_6Mg$: C, 29.23; H, 5.40; N 6.82. Found: C, 29.82; H, 5.50; N, 6.78.[12] IR bands (cm$^{-1}$) for **1** (KBr): 3452m, 3027w, 2894w, 2880w, 2869w, 1681s, 1611s, 1472w, 1374s, 1349s, 1026m, 807s.

**Preparation of Magnesium(II) Formate Dihydrate $Mg(HCOO)_2 \cdot 2H_2O$ (2).** This compound is already reported in the literature;[13] herein, an alternative synthesis is described. Magnesium perchlorate hexahydrate $Mg(ClO_4)_2 \cdot 6H_2O$ (5.27 g, 16 mmol) was dissolved together with formic acid (0.3 mL, 8 mmol) in a *N,N*-dimethylformamide (DMF)/ethanol/water mixture in the ratio 5 mL:0.5 mL:0.5 mL. The mixture was transferred to a Teflon-lined stainless steel autoclave and sealed as described above for **1**. After heating of the reactor at at 140 °C for 24 h, followed by slow overnight cooling, colorless prismatic crystals of **2** were obtained. They were collected, washed with fresh ethanol (4 × 10 mL), and dried under a nitrogen stream at room temperature. Yield: 1.38 g (58%; calculated with respect to magnesium perchlorate). The IR data obtained on our samples match to those reported previously in the literature.[13,22a] Anal. Calcd. For **2**, $C_2H_6O_6Mg$: C, 15.96; H, 3.99. Found: C, 16.13; H, 4.04. The identity of the material synthesized with the reported magnesium formate dihydrate was also confirmed by single-crystal X-ray analysis.

**X-ray Crystallographic Studies.** The XRD data for **1** were collected on Enraf-Nonius CAD4 diffractometer equipped with a graphite monochromator and Mo Kα radiation (crystal data are reported in Table 1). The intensity collected were corrected for Lorenz and polarization effects. During the data collection three standard reflections were monitored every 2 h. The atomic scattering factors are those reported by Cromer and Waber.[14] The structure was solved by direct methods using the SIR97 program.[15] The refinements were made by full matrix least squared on all $F^2$ data using SHELXL97.[16] Anisotropic thermal parameters were allotted only for the nondisordered atoms. The hydrogen atoms were found in the Fourier maps. Only the coordinates of the hydrogen atom of the formate ligand were refined. For this hydrogen atom an isotropic structure factor 20% bigger than the corresponding bonded atoms was chosen. The molecular drawing was made using the ORTEP-III program for Windows.[17] The computational work was performed using the WINGX interface.[18]

XRPD measurements were carried out with a PHILIPS X'PERT PW3020 powder diffractometer equipped with a diffracted beam graphite monochromator and operating with Cu Kα radiation. 0.5° divergence and scatter slits and a 0.1 mm receiving slit were used. The step size was 0.02° of $2\theta$ with a counting time of 1 s/step. To minimize the effect of possible preferred orientation the sample was laterally loaded into a low background aluminum sample holder with a cut quartz monocrystal underneath. High quality X-ray diffraction pattern for the hydrated phase **2a** was collected using a Panalytical X'PERT PRO equipped with the X'Celerator solid state detector in the 10 ÷ 130° $2\theta$ region. The counting time was 30 s/step.

Temperature dependent X -Ray powder diffraction spectra were collected using a Anton Paar HTK 1200N Oven camera, equipped on the right-side of the PHILIPS PW3020 diffractometer and working with a Ni filter on the diffracted beam. The heating rate was 3 °C min$^{-1}$ for all the compounds. The measurements were carried out at ambient pressure under a mild $N_2$ flow.

## Results and Discussion

**Syntheses.** Both compounds **1** and **2** were prepared using solvothermal methods, in homemade stainless steel autoclaves with an inner Teflon beaker. Originally, this methodology was applied to the synthesis of "fully inorganic" silicate materials (zeolites) and phosphates,[19] but later it was successfully used to synthesize porous metal−organic materials.[20] Traditional solution methods proved to be unsuccessful for the synthesis of the formate species, in particular if high yields of good-quality single crystals are desired. Several trials were made using different reaction conditions. For example, slow diffusion at ambient temperature through a G4 sintered glass filter of a toluene solution of triethylamine into a toluene/DMF solution containing HCOOH and magnesium perchlorate only led to few plate-like small crystals after 2 days, not suitable for XRD. Layering of a methanolic magnesium perchlorate solution over a water HCOOH solution led to white powdery products, both at ambient and low (4 °C) temperature. The protonated form of the acid is better than the carboxylate as starting material. Thus, when sodium formate is employed instead of formic acid, immediate formation of a white insoluble noncrystalline precipitate occurs. Slow deprotonation of the acid by DMF during the solvothermal syntheses is therefore crucial to get crystalline materials, as previously observed also by different authors.[21] The solvent influence was also examined. Presence of DMF is essential to get a crystalline product and to dissolve the inorganic salts thoroughly. Solvothermal attempts made either with DMF only or with a mixture of DMF/water as solvents under the same conditions led to poorer quality crystals, thus confirming that the simultaneous presence of DMF, water and ethanol provides the best results. At the temperatures chosen, DMF partially decomposes to give dimethylamine, which is eventually "trapped" inside the pores of **1**.

Variations of the stoichiometry of the reagents revealed that the final product is always the same, no matter the metal-to-ligand ratio.

Finally, the nature of the counteranion in the magnesium inorganic reagent was considered. The same results were obtained using either $Mg(ClO_4)_2 \cdot 6H_2O$ or $Mg(NO_3)_2 \cdot 6H_2O$, with no significant differences for yields or phase purity, as confirmed by the XRPD spectra of the two samples prepared from the two different magnesium salts (Figure 1). Phase **1** is never obtained pure, the impurity being unknown.[12] Phase **2** is pure, as checked through repeated syntheses under the same conditions.

The simulated powder diffraction patterns calculated from the single-crystal data show that the most intense peaks for **1**

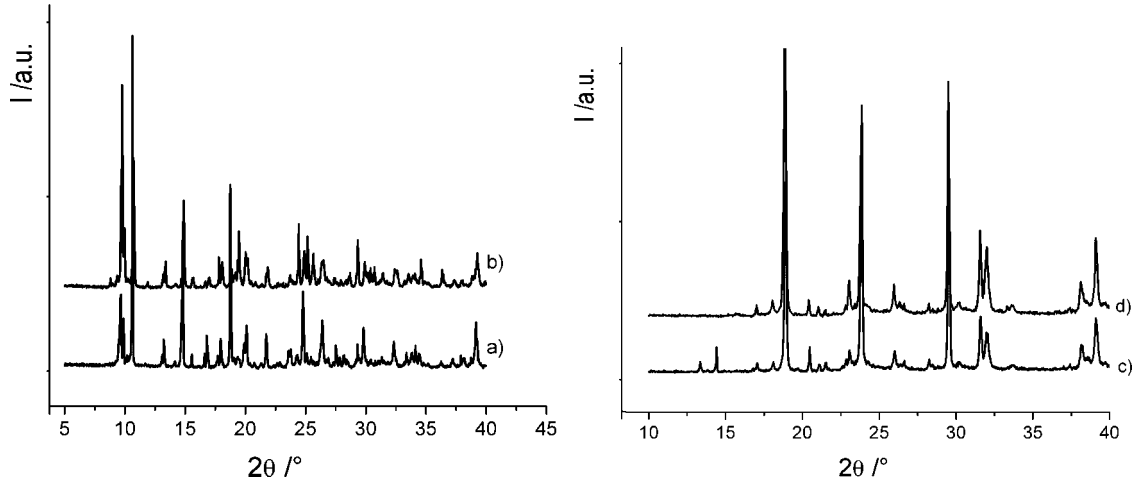


**Figure 1.** XRPD patterns of (a) **1** prepared from magnesium nitrate hexahydrate; (b) **1** prepared from magnesium perchlorate hexahydrate; (c) **2** prepared from magnesium perchlorate hexahydrate; (d) **2** prepared from magnesium nitrate hexahydrate.

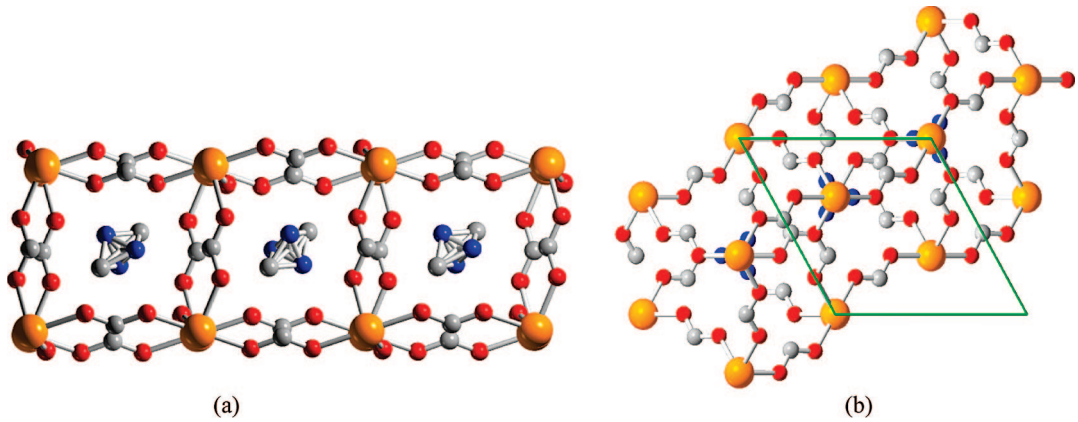


**Figure 2.** X-ray crystal structure of **1**. (a) View of the cubic cavities with Mg atoms at the corners, containing (disordered) dimethylamine molecules (view along the [011] Miller planes). (b) View along the [001] Miller planes. Atom color code: orange, magnesium; light gray, carbon; red, oxygen; blue, nitrogen. Hydrogen atoms omitted for clarity. Cell borders are drawn in light green.

appear at $2\theta = 15°$, 20° and 25°, respectively, while those of **2** fall at $2\theta = 19°$, 24°, and 29°, in close agreement with the experimental spectra shown above. As already mentioned, impurities in the $9° < 2\theta < 11°$ range are also present in **1**.

The most important parameter that influences the reaction course seems to be the DMF/$H_2O$ ratio in the solvent mixture. In the presence of a higher DMF/$H_2O$ ratio, preferred formation of the 3D network **1** is observed, while, at a lower DMF/$H_2O$ ratio, with a higher relative water content (together with a more concentrated solution with respect to the reagents), the dihydrate 2D species **2** is the main product.

**Infrared Spectral Analysis.** Infrared spectra of formates **1** and **2** (KBr pellets) showed the characteristic stretching, bending and rocking modes of the formate molecule: $\nu_{asym}$(O−C−O) at 1681−1611 (**1**)/1604 (**2**) $cm^{-1}$, $\nu_{sym}$(O−C−O) + $\delta_{asym}$(H−C−O) at 1374 (**1**)/1378 (**2**) $cm^{-1}$, $\gamma$($HCOO^-$) at 1026 (**1**)/1089 (**2**) $cm^{-1}$ and $\delta_{sym}$(O−C−O) at 807 (**1**)/819 (**2**) $cm^{-1}$. Tentative assignment of the normal modes is made referring to previous spectroscopic work present in the literature.[22] The wavenumber shift in passing from free to metal-coordinated formate mirrors the trend already observed for molecular formates:[23] in particular, both $\nu_{sym}$(O−C−O) and $\nu_{asym}$-(O−C−O) are expected to *increase* upon carboxylate coordination to Mg(II). In the case of **1**, $\nu_{sym}$(O−C−O) shifts from 1361 [in Na(HCOO)] to 1374 $cm^{-1}$, while $\nu_{asym}$(O−C−O) moves from 1617 to 1681 $cm^{-1}$.

**Structures Description.** Table 1 collects the main XRD data of **1**, while its structure is depicted in Figure 2.

The framework of **1** is the same as those of the already reported Mn, Co, Ni,[24] Zn[10] formates; nonetheless, it represents a new polymeric arrangement for (anhydrous) magnesium formate. The structure consists of a cubic polymeric network in which the vertices are occupied by Mg atoms. Magnesium coordination sphere is almost perfectly octahedral. The formate molecule is bridging adjacent metal centers in an *antianti* coordination mode, according to the nomenclature used by Gao et al.[24] The cubic cavities are occupied by the disordered dimethylamine molecules, deriving from partial decomposition of DMF solvent under the used solvothermal conditions. The Mg−O [2.0901(1) Å] and the O−C distances [1.237(2) Å], as well as the Mg−O−C [129.3(1)°] and O−C−O [127.1(2)°] angles are in the range of the corresponding distances and angles of other published magnesium formate systems.[5i]

A picture of the two-dimensional structure of **2** is reported below (Figure 3). Planes made of polymeric $Mg(HCOO)_2$ moieties are interconnected through hydrogen bonding between the two axial aquo ligands on magnesium and the formate ligands of the neighboring (upper and lower) sheets. The reader may refer to the cited article[13] for further structural details.

**Thermal Behavior.** The results coming from the TG-DTA of **1** supported the assignment of its molecular formula as

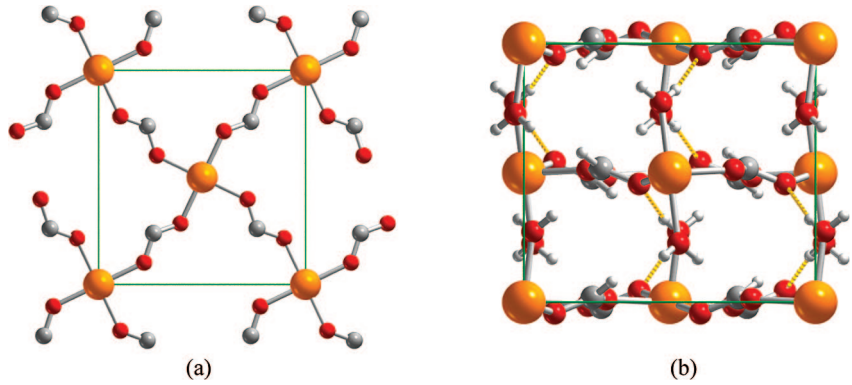


**Figure 3.** X-ray crystal structure of **2** (from ref 13). (a) View of the 2D network made of infinite $Mg(HCOO)_2$ sheets (view along the [001] Miller planes, axial aquo ligands and hydrogen atom on formate removed for clarity). (b) View along the [010] Miller planes, showing the complex hydrogen bonding between the axial aquo ligands and the formate ions on the adjacent planes. Atom color code: orange, magnesium; light gray, carbon; red, oxygen. Cell borders are drawn in light green. Hydrogen bonding is drawn in yellow.

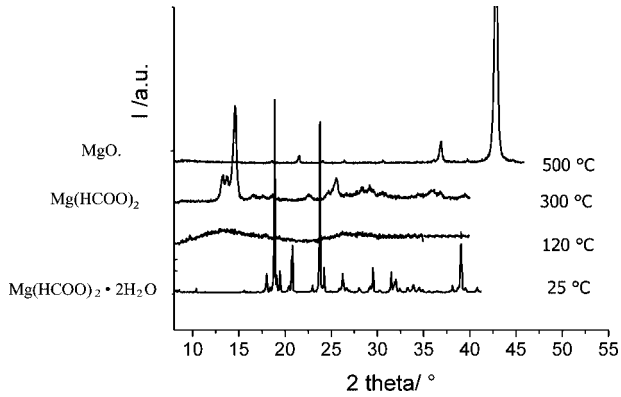


**Figure 4.** Temperature-dependent XRPD patterns for **2**. The temperatures and the corresponding products are also indicated in the graphs.

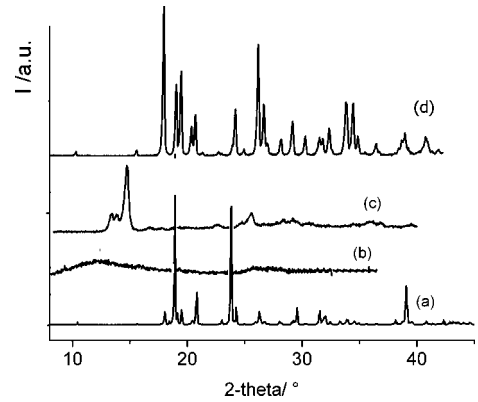


**Figure 5.** XRPD patterns of **2** (a), amorphous domain at 120−140 °C (b), $\mathbf{2}_{act}$ (activated at 300 °C) (c), and water-regenerated phase **2a** (d).

$Mg(HCOO)_2(HCOOH) \supset (CH_3)_2NH$ instead of $[(CH_3)_2NH_2][Mg(\mu\text{-}HCOO)_3]$. In fact, an initial weight loss of ca. 22% is consistent with the only dimethylamine elimination [corresponding to the $Mg(HCOO)_2(HCOOH) \supset (CH_3)_2NH \rightarrow Mg(HCOO)_2(HCOOH)$ transformation, which reaches completion at 260 °C]. As a consequence, formation of a "salt-like" species, where a proton is transferred from the acid to the amine, is to be excluded. Complete conversion to MgO is reached at 470 °C. Since compound **1** could not be obtained pure, the following discussion will be limited only to the hydrate phase **2**, for which pure samples could be synthesized. The thermal X-ray spectra for **2** are shown in Figure 4.

As already observed by Malard and co-workers,[13] in the TG-DTA analysis no weight loss is observed for **2** up to 120 °C. The first weight change (24%) is found between 120 and 140 °C and corresponds to the loss of two water molecules (calcd. 24%). A *plateau* can be observed up to 380 °C, before a severe weight loss of 50% occurs, which can be ascribed to the $Mg(HCOO)_2 \rightarrow MgO$ transformation (calcd. 49.3%). In agreement with the *plateau* in the thermogravimetric curve, the diffraction pattern collected at 300 °C shows the existence of a *crystalline* phase, whose calculated formula from TG measurement is consistent with the formula $Mg(HCOO)_2$. On increasing the temperature above 400−450 °C, loss of water and carbon monoxide leaves MgO as the last phase at the end of the analysis. The high thermal stability of **2** mirrors that observed in similar compounds previously synthesized.[4a,5i]

**Dehydration and Rehydration of 2: A Phase Transition.** In order to determine if *anhydrous* magnesium formate coming from thermal activation of **2** could interact again with water to form a guest-inclusion species after guest vapor diffusion into the hosting framework, the activated phase was put into a closed desiccator, and exposed to vapors of $H_2O$ under reduced pressure and at ambient temperature. The experiment was successful, but, instead of regenerating compound **2**, a *different 3D* dihydrate species (**2a**) appeared. Activation of **2** was achieved at 300 °C, yielding an activated phase $\mathbf{2}_{act}$ with very poor crystallinity degree (see Figure 5b), which could not be indexed. As observed from the TGA measurements, in this case the activated phase should correspond to the $Mg(HCOO)_2$ "anhydrous" open framework. The hydrate **2a** was also obtained after soaking $\mathbf{2}_{act}$ into *liquid* water for 1 h, and its diffraction pattern is shown in Figure 5c. Its structure was successfully indexed, finding the following cell parameters: $a = 8.6528$, $b = 7.163$, $c = 9.4067$ Å, $\beta = 98.012°$, space group = $P2_1/c$, M(20) = 23. Additional experimental evidence inferred from independent measurements on zinc formates[25] suggested that this species could be isostructural to *Lipton's zinc formate dihydrate*.[5a] Thus, the structure of **2a** was refined using the Rietveld method implemented in the program GSAS,[26] starting from Lipton's phase and replacing magnesium with zinc in the framework. The final Rietveld plot and the resulting structure are shown in Figure 6. Structural refinement confirmed the perfect crystal system analogy between **2a** and zinc(II) formate dihydrate.[5a] The network is constituted by two different

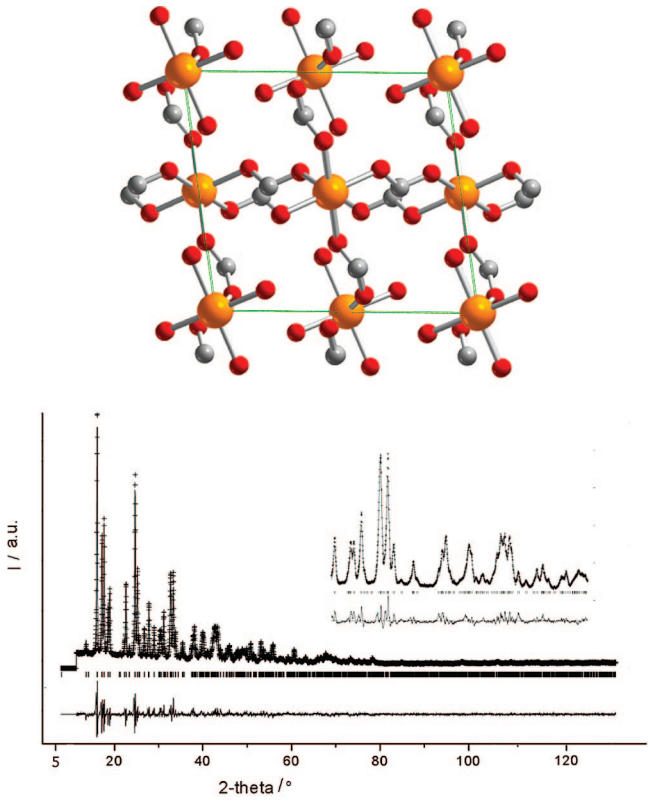


**Figure 6.** Structure representation and final Rietveld plot for **2a**. The inset shows a zoom of the 30−50° 2$\theta$ region. Atom color code: orange, magnesium; light gray, carbon; red, oxygen. Hydrogen atoms are omitted for clarity. Cell borders are drawn in light green.

magnesium sites: in the first one the metal center is coordinated to six different (bridging) formates, while the second one shows four aquo ligands occupying the equatorial positions and only two (bridging) formates on the axial positions. Thus, the overall formula could also be written as $[Mg(HCOO)_2 \cdot Mg(H_2O)_4(HCOO)_2] \equiv 2[Mg(HCOO)_2 \cdot 2H_2O]$.

This 2D to 3D phase transition is not very common among coordination compounds, and it represents, to the best of our knowledge, the very first transition of this kind observed. The process is "*quasi-reversible*", in the sense that the dehydration/rehydration process is feasible, but the initial and final products are not structurally identical. They indeed represent two *polymorphs* of the same compound. Scheme 1 highlights the transformation described. The last part of the process is totally reversible: upon heating, **2a** is converted again into $\mathbf{2}_{act}$, as checked through PXRD.

**Gas Sorption Studies: $CO_2$ Adsorption Isotherms.** The adsorption behavior of (preactivated) **2** was tested using $CO_2$, in order to clarify the possible role of these compounds as gas storage materials. Different activation temperatures were chosen in order to investigate the adsorptive properties of the different phases. **2** was activated at 300 °C to form the phase $\mathbf{2}_{act}$. The results obtained from the $CO_2$ adsorption at 25 °C are reported in Figure 7.

$CO_2$ adsorption isotherms were recorded at 25 °C, following the procedure recently described by Millward and Yaghi.[27] Unfortunately, $CO_2$ adsorption could not be studied at pressure higher than atmospheric, because the available instrument has a maximum dosing pressure of 800 torr. Notably, during $CO_2$ adsorption experiments on metal−organic framework materials,[27] a *plateau* is usually reached but at a higher pressure (at least above 10 bar, depending from the pore size of the material)

**Scheme 1. A 2D-to-3D Phase Transition in the Dehydration Rehydration Cycle of Magnesium Formate**

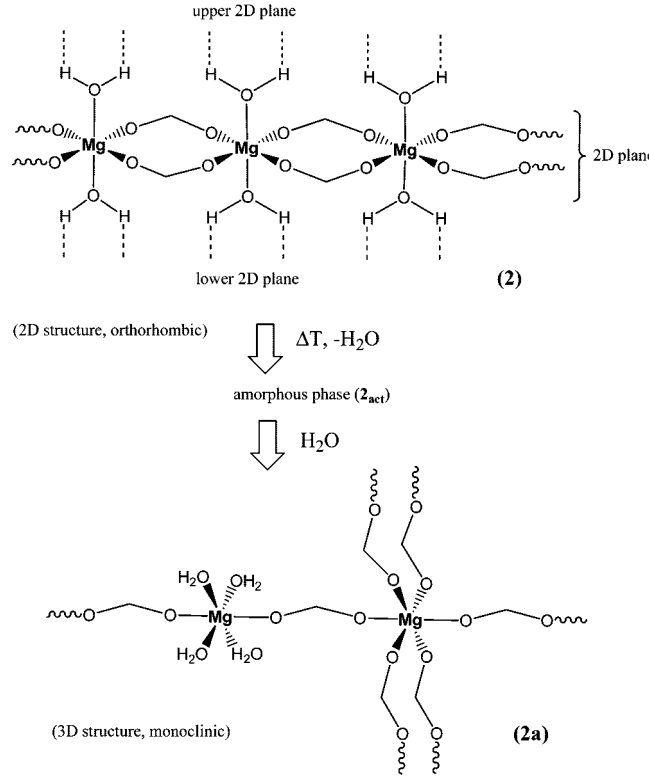


than that achievable by the instrument used in this study. Although the pressure reached during our experiments is only a little below the atmospheric pressure, the differences observed in the adsorption behavior may be considered indicative of the different ability of the materials to store $CO_2$. The highest value is obtained with **2** activated at 120 °C, where 1.32 wt% $CO_2$ is stored at ambient temperature and $p_{CO_2} = 700$ torr. After degassing of **2** at 300 °C to form the $\mathbf{2}_{act}$ phase, a slight decrease in the adsorbed amount of $CO_2$ is observed. Although XRPD measurements confirmed that the $\mathbf{2}_{act}$ phase is preserved after $CO_2$ adsorption experiments, a partial *pore collapse* cannot be excluded, induced by the prolonged heating under vacuum. In fact, this treatment is more "severe" than that used during both TG and temperature-dependent XRPD analyses. This fact could account for the reduction of the $CO_2$ adsorption. Notably, the adsorption process is *fully reversible*. In fact, a sequence of $CO_2$ adsorption experiments have been performed on the $\mathbf{2}_{act}$ phase with intermediate degassing treatment at 25 °C from 12 h to 30 min. In all cases, adsorption isotherms have been reproduced reasonably well. The strong carbon dioxide uptake of $\mathbf{2}_{act}$ is probably due to the highly ionic character of the Mg−O bond, which induces a strong interaction with the polar C═O bonds present in $CO_2$. The adsorption properties of the Mg-derivative are currently under a more detailed investigation, in order to fully understand its behavior as gas storage material.

## Conclusions and Outlook

Two polymeric magnesium formates **1** and **2** have been prepared by solvothermal syntheses of simple salts with formic acid in DMF/EtOH/$H_2O$ mixtures and thoroughly analyzed. They are polymorphs, and in the case of **1** the cubic network topology has been found for the first time. The hydrate form **2** undergoes an unexpected crystal-to-crystal phase transition when heated and soaked back into water. The final hydrate phase **2a** is monoclinic, while the starting material is orthorhombic.

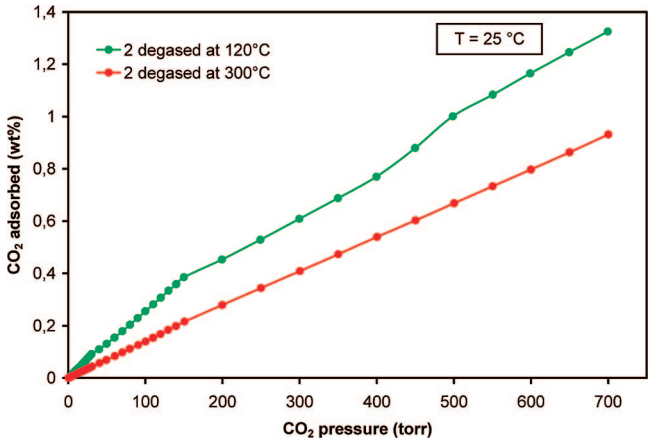


**Figure 7.** $CO_2$ adsorption isotherms recorded for **2** after suitable degassing treatments.

Beyond their interest as coordination polymers, possible applications in the fields of gas sensing and *selective* guest inclusion have been investigated. In fact, preliminary host−guest experiments carried out on $\mathbf{2_{act}}$ using different solvents (MeOH, *i*-PrOH, THF, DMF, and MeCN) showed that it always reacts in the same fashion producing **2a**, as checked through XRPD. This implies that $\mathbf{2_{act}}$ is *selective for $H_2O$ adsorption* when put into a solvent/water mixture (i.e., a "wet" solvent). The ability at trapping selectively $H_2O$ could envisage a possible application of these materials as dehydrating agents.

Both chemi- and physisorption are quite limited. The compact structure with small available inner surface area in the 3D scaffold (when present) limits gas adsorption, while the lack of energy-suitable frontier orbitals on Mg(II), able to split $CO_2$, hampers chemisorption. Gas adsorption experiments showed that **2** possesses good sorption ability. These preliminary results suggest that, after activation, **2** could show interesting properties in the light and polar molecules storage field. The adsorption behavior of $\mathbf{2_{act}}$ toward other light gases (such as $H_2$, $O_2$, $CH_4$, and CO) is currently under investigation, with the aim of applying these molecules to the important field of *gas separation* methodologies.[28]

The formate molecule is very small and possesses a strong coordinating ability, thus tending to form high-density materials. The logical extension in this direction currently pursued in our laboratories is to try to enlarge the pore size. This may be achieved by introducing additional ligands (such as tertiary amines) in the molecular structure. As a result, a hybrid material featuring a different supramolecular assembly, where the formate anion "co-crystallizes" together with the amine, should be formed. Alternatively, pore enlargement could be accomplished by using longer aliphatic open-chain acids, under the same reaction conditions. Other lightweight metals such as calcium, titanium or aluminum will be also investigated to verify whether their formate salts may provide further improvement in these areas.

**Acknowledgment.** A.R. and M.P. acknowledge the *motu proprio* FIRENZE HYDROLAB project by Ente Cassa di Risparmio di Firenze (http://www.iccom.cnr.it/hydrolab/) for funding this research activity, through a postdoctoral grant to A.R. T.M. and P.F. acknowledge University of Trieste, FISR2002 *"Nanosistemi inorganici ed ibridi per l'innovazione di celle a combustibile"* and INSTM for financial support. A.R. would like to thank Dr. Stefano Midollini and Mr. Carlo Bartoli at ICCOM-CNR, the former for very fruitful discussions and the latter for making the autoclaves used for solvothermal syntheses.

**Supporting Information Available:** X-ray crystallographic information files (CIF) for **1** (CCDC no. 696736) and **2a** (CCDC no. 696737). These materials are available free of charge via Internet at http://pubs.acs.org.

## References

(1) (a) Kahn, O. *Acc. Chem. Res.* **2000**, *33*, 647. (b) Li, Y.-G.; Hao, N.; Wang, E.-B.; Lu, Y.; Hu, C.-W.; Xu, L. *Eur. J. Inorg. Chem.* **2003**, 2567.

(2) (a) Fujita, M.; Kwon, Y.-J.; Washizu, S.; Ogura, K. *J. Am. Chem. Soc.* **1994**, *116*, 1151. (b) Seo, J.-S.; Whang, D.; Lee, H.; Jun, S. I.; Oh, J.; Jeon, Y. J.; Kim, K. *Nature* **2000**, *404*, 982.

(3) (a) Recent reviews for gas storage on coordination polymers : Kitagawa, S.; Kitaura, R.; Noro, S.-I. *Angew. Chem., Int. Ed.* **2004**, *43*, 2334. (b) Seayad, A. M.; Antonelli, D. M. *Adv. Mater.* **2004**, *16*, 765. (c) Rowsell, J. L. C.; Yaghi, O. M. *Angew. Chem., Int. Ed.* **2005**, *44*, 4670.

(4) (a) Lu, J. Y.; Babb, A. M. *Chem. Commun.* **2002**, 1340. (b) Dybtsev, D. N.; Chun, H.; Kim, K. *Angew. Chem., Int. Ed.* **2004**, *43*, 5033. (c) Ohmori, O.; Kawano, M.; Fujita, M. *J. Am. Chem. Soc.* **2004**, *126*, 16292. (d) Choi, H. J.; Suh, M. P. *J. Am. Chem. Soc.* **2004**, *126*, 15844. (e) Hermes, S.; Schroeter, M.-K.; Schmid, R.; Khodeir, L.; Mulher, M.; Tissler, A.; Fischer, R. W.; Fischer, R. A. *Angew. Chem., Int. Ed.* **2005**, *44*, 6237. (f) Chen, B.; Liang, C.; Yang, J.; Contreras, D. S.; Clancy, Y. L.; Lobkovsky, E. B.; Yaghi, O. M.; Dai, S. *Angew. Chem., Int. Ed.* **2006**, *45*, 1390. (g) Wang, Z.; Zhang, Y.; Kurmoo, M.; Liu, T.; Vilminot, S.; Zhao, B.; Gao, S. *Aust. J. Chem.* **2006**, *59*, 617. See also refs 5e and 5i.

(5) (a) Lipton, A. S.; Smith, M. D.; Adams, R. D.; Ellis, P. D. *J. Am. Chem. Soc.* **2002**, *124*, 410. (b) Lu, J. Y.; Babb, A. M. *Chem. Commun.* **2002**, 1340. (c) Baggio, R.; Stoilova, D.; Garland, M. T. *J. Mol. Struct.* **2003**, *659*, 35. (d) Dybstev, D. N.; Chun, H.; Yoon, S. H.; Kim, D.; Kim, K. *J. Am. Chem. Soc.* **2004**, *126*, 32. (e) Wang, Z.; Zhang, B.; Fujiwara, H.; Kobayashi, H.; Kurmoo, M. *Chem. Commun.* **2004**, 416. (f) Viertelhaus, M.; Anson, C. E.; Powell, A. K. *Z. Anorg. Allg. Chem.* **2005**, *631*, 2365. (g) Viertelhaus, M.; Adler, P.; Clérac, R.; Anson, C. E.; Powell, A. K. *Eur. J. Inorg. Chem.* **2005**, 692. (h) Wang, Z.; Zhang, B.; Kurmoo, M.; Green, M. A.; Fujiwara, H.; Otzuka, T.; Kobayashi, H. *Inorg. Chem.* **2005**, *44*, 1230. (i) Rood, J. A.; Noll, B. C.; Henderson, K. W. *Inorg. Chem.* **2006**, *45*, 5521. (j) Guo, J.-Y.; Zhang, T.-L.; Zhang, J.-G. *Chin. J. Chem.* **2006**, *24*, 745. (k) Wang, Y.; Cao, R.; Bi, W.; Li, X.; Yuan, D.; Sun, D. *Microporous Mesoporous Mater.* **2006**, *91*, 215. (l) Samsonenko, D. G.; Kim, H.; Sun, Y.; Kim, G.-H.; Lee, H.-S.; Kim, K. *Chem. Asian J.* **2007**, *2*, 484. (m) Tian, Y.-Q.; Zhao, Y.-M.; Xu, H.-Y.; Chi, C.-Y. *Inorg. Chem.* **2007**, *46*, 1612. (n) Su, J.; Wang, Y.; Yang, S.; Li, G.; Liao, F.; Lin, J. *Inorg. Chem.* **2007**, *46*, 8403. (o) Wang, Z.; Zhang, X.; Batten, S. R.; Kurmoo, M.; Gao, S. *Inorg. Chem.* **2007**, *46*, 8439.

(6) (a) Selected examples of molecular formates include $Cu(HCOO)_2 \cdot 4H_2O$ . Kiriyama, R.; Ibamoto, H.; Matsuo, K. *Acta Crystallogr.* **1954**, *7*, 482. (b) $In(HCOO)_3$. Habeeb, J. J.; Tuck, D. G. *J. Chem. Soc., Dalton Trans.* **1973**, *3*, 243. (c) Actinide formates. Casellato, U.; Vigato, P.; Vidali, M. *Coord. Chem. Rev.* **1978**, *26* (2), 85. (d) $Cd(HCOO)_2 \cdot 2H_2O$. Honkonen, R. S.; Ellis, P. D. *J. Am. Chem. Soc.* **1984**, *106*, 5488. (e) $Co(HCOO)_2 \cdot 2H_2O$. Arii, T.; Kishi, A. *Thermochim. Acta* **1999**, *325*, 157. (f) Rb(HCOO) and Cs(HCOO) . Wilson, M. P.; Alcock, N. W.; Rodger, P. M. *Inorg. Chem.* **2006**, *45*, 4539.

(7) (a) Braga, D.; Grepioni, F.; Desiraju, G. R. *Chem. Rev.* **1998**, *98*, 1375. (b) Moulton, B.; Zawrotoko, M. J. *Chem. Rev.* **2001**, *101*, 1629. (c) Seddon, K. R. *Cryst. Growth Des.* **2004**, *4*, 1087. (d) Nangia, A. *Cryst. Growth Des.* **2006**, *6*, 4.

(8) (a) Doyle, R. P.; Nieuwenhuyzen, M.; Kruger, P. E. *CrystEngComm* **2006**, *8*, 904. (b) Fu, S.-J.; Cheng, C.-Y.; Lin, K.-J. *Cryst. Growth Des.* **2007**, *7*, 1381.

(9) (a) Eddaoudi, M.; Moler, D. B.; Li, H. L.; Chen, B. L.; Reineke, T. M.; O'Keeffe, M.; Yaghi, O. M. *Acc. Chem. Res.* **2001**, *34*, 319. (b) Janiak, C. *Dalton Trans.* **2003**, 2781. (c) Rather, B.; Zaworotko, M. J. *Chem. Commun.* **2003**, 830. See also refs 7a,b, and references therein.

(10) Clausen, H. F.; Poulsen, R. D.; Bond, A. D.; Chevallier, M.-A. S.; Iversen, B. B. *J. Solid State Chem.* **2005**, *178*, 3342.

(11) An interesting review on the last advances in the XRPD technique is available, see Harris, K. D. M.; Cheung, E. Y. *Chem. Soc. Rev.* **2004**, *33*, 526.

(12) A comparison of the calculated XRPD spectrum (simulated from the single-crystal data) with the experimental spectrum recorded on the solid product showed that, in the case of the zinc nitrate synthesis, some impurities are present, whose relative amount is presumably very

small (less than 10%) with respect to the main phase. This can be inferred from the satisfactory match of the measured elemental analyses with the theoretical ones. Products from zinc perchlorate are generally less pure than those coming from nitrate, probably up to 40−50%, from the X-ray intensities (Figure 1, spectrum b).

(13) Malard, C.; Pezerat, H.; Herpin, P.; Toledano, P. *J. Solid State Chem.* **1982**, *41*, 67.

(14) Cromer, D. T.; Waber, J. T. *Acta Crystallogr.* **1965**, *18*, 104.

(15) Altomare, A.; Burla, M. C.; Cavalli, M.; Cascarano, G. L.; Giavovazzo, C.; Gagliardi, A.; Moliterni, A. G. G.; Polidori, G.; Spagna, R. *J. Appl. Crystallogr.* **1999**, *32*, 115.

(16) Sheldrick, G. M. *Program SHELXL97 (crystal structure refinement*); University of Göttingen: Göttingen, Germany, 1997.

(17) (a) *ORTEP-III*. Burnett, M. N.; Johnson, C. K. Report ORNL-6895; Oak Ridge National Laboratory: Oak Ridge, TN, 1996; (b) Farrugia, L. J. *J. Appl. Chem.* **1997**, *30*, 565.

(18) Farrugia, L. J. *J. Appl. Chem.* **1999**, *32*, 837.

(19) (a) Thomas, J. M.; Thomas, W. J. *Princ. Pract. Heterogen. Catal.* **2003**, *216*, 298, and references therein. (b) Cundy, C. S.; Cox, P. A. *Chem. Rev.* **2003**, *103*, 663. (c) Corma, A. *J. Catal.* **2003**, *216*, 298.

(20) (a) Some early examples of solvothermal (or hydrothermal) syntheses applied to MOFs are the following: Yaghi, O. M.; Li, H. *J. Am. Chem. Soc.* **1995**, *117*, 10401. (b) Yaghi, O. M.; Li, G.; Groy, T. L. *J. Solid State Chem.* **1995**, *117*, 256. (c) Yaghi, O. M.; Li, G.; Li, H. *Nature* **1995**, *378*, 703. (d) Yaghi, O. M.; Li, H.; Groy, T. L. *J. Am. Chem. Soc.* **1996**, *118*, 9096. (e) Yaghi, O. M.; Li, H.; Groy, T. L. *Inorg. Chem.* **1997**, *36*, 4292.

(21) Roswell, J. L. C.; Yaghi, O. M. *Microporous Mesoporous Mater.* **2004**, *73*, 3.

(22) (a) Stoilova, D.; Koleva, V. *J. Mol. Struct.* **2000**, *553*, 131. (b) Stoilova, D. *J. Mol. Struct.* **2006**, *798*, 141. (c) Stoilova, D.; Baggio, R.; Garland, M. T.; Marinova, D. *J. Mol. Struct.* **2007**, *842*, 67.

(23) Donaldson, J. D.; Knifton, J. F.; Ross, S. D. *Spectrochim. Acta* **1964**, *20*, 547.

(24) Wang, X-Y.; Gan, L.; Zhang, S.-W.; Gao, S. *Inorg. Chem.* **2004**, *43*, 4615.

(25) Rossin, A. ICCOM-CNR, unpublished results.

(26) *GSAS*; Larson, C., von Dreele, R. B. *Generalized Crystal Structure Analysis System*; Los Alamos National Laboratory: New Mexico, 2001. Rietveld refinement of **2a** was performed using the *GSAS* program. Firstly, zero shift, cell parameters, background, and profile shape were refined; a corrected pseudo-Voigt profile function (six terms) with two terms for the correction of asymmetry at the low-angle region was used. Secondly, atomic coordinates and isotropic thermal factors were refined restraining the distances and the angles to the following values: Mg−O = 2.05(5) Å, C−O = 1.23(2) Å, O−C−O = 120(1)°. The statistical weight of these restraints was decreased as the refinement proceeded, but it was not possible to set it to zero, due to some unrealistic light atom bond distances. At the end of the refinement, the shifts in all parameters were less than their standard deviations. Crystal data and refinement details for **2a**: Monoclinic $P2_1/c$; $a$ = 8.6511(3), $b$ = 7.1522(3), $c$ = 9.4041(4) Å, $\beta$ = 98.166(3)°, $V$ = 575.97(4) Å$^3$; $2\theta$ range for data collection: 5−130°; no. of data = 6976, no. of reflections = 2072; $R_F2$ = 0.080, $Rwp$ = 0.097, $Rp$ = 0.071 ($R_F2 = \Sigma |F_o^2 - F_c^2| / \Sigma |F_o|^2$; $Rp = \Sigma |I_o - I_c| / \Sigma I_o$; $Rwp = [\Sigma w(I_o - I_c)^2 / \Sigma w I_o^2]^{1/2}$).

(27) (a) Millward, A. R.; Yaghi, O. M. *J. Am. Chem. Soc.* **2005**, *127*, 17998. (b) Walton, K. S.; Millward, A. R.; Dubbeldam, D.; Frost, H.; Low, J. J.; Yaghi, O. M.; Snurr, R. Q. *J. Am. Chem. Soc.* **2008**, *130*, 406.

(28) Unpublished $H_2$ adsorption experiments on **2** showed that in this case performance is much worse than with $CO_2$. A maximum value of 0.070 wt% (corresponding to 0.347 mmol/g) of hydrogen adsorbed at−196 °C and at $p_{H_2}$ = 700 torr was recorded. Thus, *selective* gas sorption (i.e., gas *separation*) in a $H_2/CO_2$ mixture is achievable with **2**.

CG800181Q